13.3

Peculiarities of Photoelectron Spectra of Ge Implanted with Na^+ Ions

© S.T. Abraeva, D.A. Tashmukhamedova, M.B. Yusupjanova, B.E. Umirzakov

Tashkent State Technical University, Tashkent, Uzbekistan
E-mail: ftmet@mail.ru

Received July 18, 2022
Revised September 5, 2022
Accepted November 2, 2022

Using the methods of Auger electron and photoelectron spectroscopy and light absorption spectroscopy, the composition, densities of state of electrons in the valence band, and parameters of the energy bands of Ge (111) implanted with Na^+ ions with an energy of $E_0 = 0.5$ keV at a dose of $D_{sat} = 6 \cdot 10^{16}$ cm^{-2} and a thin layer of $NaGe_2$ obtained by annealing ion-implanted Ge. It is shown that a narrow *n*-type band (~ 0.2 eV) appears in the Ge valence electron spectrum after ion implantation near the bottom of the conduction band, which is explained by the presence of a large number of unbound Na atoms in the ion-implanted layer. $NaGe_2$ nanofilms with a band gap of ~ 0.45 eV was obtained for the first time by annealing ion-implanted Ge.

Keywords: nanostructure, photoelectrons, Auger electron spectroscopy, absorption spectrum, hybridized states, electron state densities, ion implantation.

DOI: 10.21883/TPL.2023.01.55342.19311

Germanium nanostructures have potential applications for electronic flash memories [1,2] and light emitters in visible [3] and near-infrared [4] ranges, making this indirect-gap semiconductor attractive for novel electronic and optical devices. Compared to bulk Ge, nanocrystals exhibit a tunable emission wavelength [5] and increased oscillator strength due to the quantum confinement of excitons.

The composition, structure, and photovoltaic and optical properties of nanoscale systems based on Ge nanofilms and quantum dots produced by molecular beam epitaxy [1,6,7], thermal deposition [8,9], and ion implantation [10–13] have already been studied thoroughly. Specifically, the feasibility of production of a plasmonic composite Ag:GeSi material on a *c*-Si substrate under sequential high-dose implantation of Ge^+ and Ag^+ ions has been examined for the first time in [11]. The implantation with Ge^+ ions is accompanied by amorphization of the Si layer surface with the formation of a fine-grain composite GeSi layer. It was demonstrated in [8] that the bandgap width of nanocomposite Ge films may be adjusted in a controlled manner without any additional processing (annealing, irradiation, etc.) by varying the percentage ratio of amorphous and crystalline phases in these films, which is done by setting a specific film fabrication regime.

The electronic structure and physical properties of nanoscale $MeSi_2$-type structures produced in Si by ion implantation [14–18] and molecular beam epitaxy [19] are also characterized well at this point. However, results of experimental studies into the influence of low-energy implantation of ions of active metals on the composition, the densities of states of valence electrons, and the band parameters of Ge are still lacking.

The present study is focused on the process of production and on the electronic and crystal structure of nanoscale $NaGe_2$ objects formed on a Ge surface by Na^+ ion implantation with subsequent annealing.

Single-crystalline Ge(111) *p*- (with a boron concentration of $\sim 5 \cdot 10^{18}$ cm^{-3}) and *n*-type (with a phosphorus concentration of $\sim 10^{16}$ cm^{-3}) samples $10 \times 10 \times 0.5$ mm in size were studied. Prior to ion bombardment, the surface of Ge was degassed at $T = 1000$ K for 4–5 h in combination with short-term annealing to $T = 1200$ K in vacuum no worse than 10^{-7} Pa.

Na^+ ions with energies ranging from 0.5 to 5 keV at saturation dose $D = D_{sat} = (6-8) \cdot 10^{16}$ cm^{-2} were used for implantation. Nickel boats filled with sodium chromates served as sources of sodium. Sodium vapor was produced when these nickel boats were heated, and a certain fraction of it reached the surface of a hot tungsten spiral and became ionized. The main study was carried out at $E_0 = 0.5$ keV.

Auger electron spectroscopy (AES), ultraviolet photoelectron spectroscopy (UVPS), and measurements of the intensity of light transmitted through a sample (light absorption spectroscopy) were performed. Photon energy $h\nu$ varied within the 0.2–1.5 eV range ($\lambda \approx 6200-800$ nm). The depth (h) distribution profiles of atoms were determined by AES in combination with layer-by-layer etching of the surface by Ar^+ ions with $E_0 = 2$ keV under an angle of 5–10° to the sample surface. The depth of AES and UVPS analysis is $\sim 5-10$ Å.

The spectra (energy distribution curves, EDCs) of photoelectrons of „pristine" *p*- and *n*-type Ge samples obtained at $h\nu = 10.8$ eV are shown in Fig. 1. Electron binding energy E_b was measured from valence band top E_v. The positions of Fermi level E_F were determined relative to the Fermi level of pure Pd mounted within the target assembly. It follows from Fig. 1 that these curves have a well-pronounced structure. They represent approximately the distribution of density of states of valence-band electrons. The main

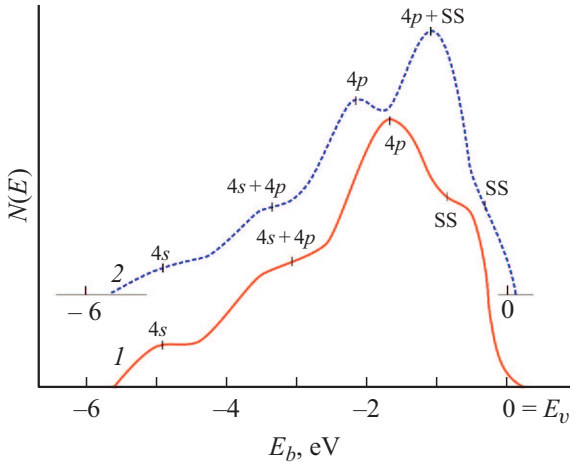

Figure 1. Normalized energy distribution of photoelectrons for Ge single crystals. *1* — *p*-type, *2* — *n*-type. $h\nu = 10.8$ eV. SS — surface states.

Table 1. Φ, φ E_g, and χ values (in eV) for *p*- and *n*-type Ge

Parameter	Ge(111)	
	p-type	*n*-type
Φ	5.3	5.1
φ	5.0	4.8
E_g	0.7	0.7
χ	4.6	4.4

Note. Parameters of energy bands were determined with an error of ~ 0.05 eV.

features for both *p*- and *n*-type Ge may be associated with the excitation of electrons from $4s$, $4p$, and hybridized $4s$ and $4p$ states of valence electrons of Ge. The feature within at $E_b = 0-0.5$ eV is attributable to the process of photoemission of electrons from surface states. These spectra were used to determine the main parameters of energy bands, which are listed in Table 1 ($\Phi = E_v$ is the photoelectric work function, $\varphi = E_F$ is the thermionic work function, E_g is the bandgap width, and χ is the electron affinity). The value of Φ was calculated as $\Phi = h\nu - \Delta E$, where ΔE is the total EDC width of photoelectrons.

Figure 2 shows the EDCs of photoelectrons for face (111) of *p*-type Ge implanted with Na ions with energy $E_0 = 0.5$ keV at $D = 6 \cdot 10^{16}$ cm^{-2} before and after annealing. It is evident that ion implantation induces significant changes in the structure and shape of the spectrum. These changes are related primarily to disordering of surface layers, the formation of nonstoichiometric Na_xGe_y germanides, and the presence of unbound Na and Ge atoms. The area under the EDC (i.e., the quantum yield of photoelectrons) increases by a factor of almost two as a result, and well-marked features at energies $E_b = -5.9$, -4.3, -2.9, -1.2, -0.3, and $+0.4$ eV relative to the valence band top emerge in dependence $N(E)$. The obtained spectra suggest that the detected peak at $E_b = -5.9$ eV corresponds to germanium, while the peak at -0.3 eV is related to unbound sodium atoms. Maxima in the Ge bandgap with $E_b = 0.4$ eV are also attributable to the presence of excess Na atoms, which leads to the formation of a narrow *n*-type band near the conduction band bottom (E_c) of germanium. All the remaining peaks (-4.3, -2.9, and -1.2 eV) correspond to nonstoichiometric sodium germanide. The majority (60–70%) of sodium atoms form chemical compounds with matrix atoms. Following 30–40 min of annealing at $T = 800$ K, almost all Na atoms form chemical bonds with Ge atoms, and a $NaGe_2$-type germanide with a thickness of 25–30 Å is produced. Intense peaks with $E_b = -1$, -3.2, and -5.1 eV and features in the region of -1.8 eV emerge in the process in EDCs of photoelectrons, while the peak associated with the impurity band vanishes. The probable interpretation of peaks is indicated next to curves.

Figure 3 presents the dependences of relative intensity of light transmitted through the sample (absorption spectrum) on photon energy $h\nu$ within the 0.2–1.0 eV interval for Ge and Ge with a $NaGe_2$ film. It can be seen that intensity $I(h\nu)$ for Ge (111) remains virtually unchanged through to $h\nu = 0.6$ eV, but then drops rapidly to zero within the $h\nu = 0.6-0.8$ eV interval. Extrapolating this section of the curve to axis $h\nu$, one obtains an estimate of E_g. In the case of a $NaGe_2$ film, I decreases rapidly within the $h\nu = 0.4-0.5$ eV interval. It can be seen from Fig. 3 that E_g assumes a value of 0.71 eV for Ge (111) and 0.45 eV for $NaGe_2$. The $I(h\nu)$ spectrum also provides an opportunity to estimate light reflection coefficient $R = 1-I$. The value of

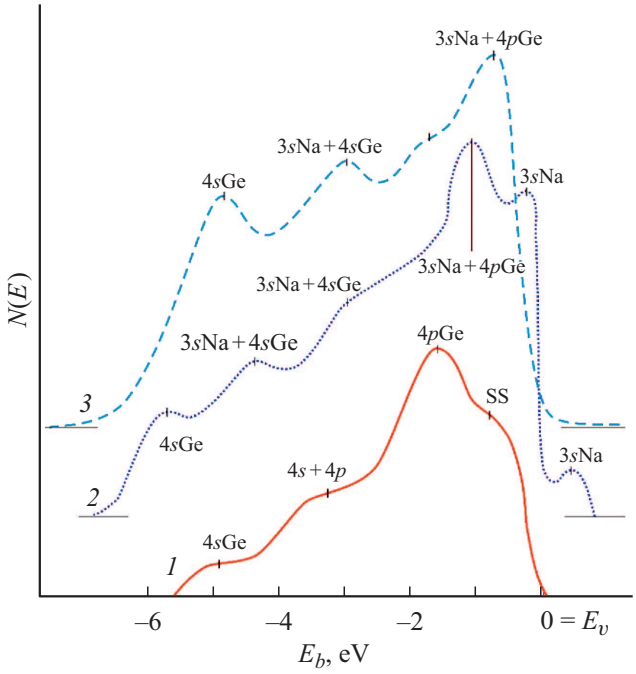

Figure 2. EDCs of photoelectrons for „pristine“ Ge (*1*) and Ge (111) implanted with Na^+ ions with $E_0 = 0.5$ keV at $D = 6 \cdot 10^{16}$ cm^{-2} before (*2*) and after annealing at $T = 800$ K (*3*).

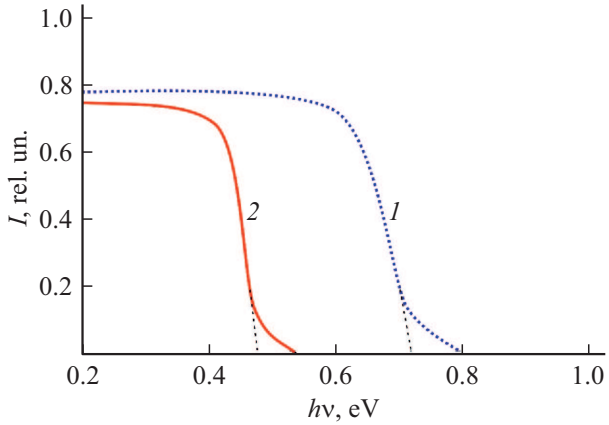

Figure 3. Dependences of light intensity I transmitted through the sample on photon energy $h\nu$. *1* — Ge (111), *2* — $NaGe_2$/Ge film.

Table 2. Values of the main parameters (in eV) of the band structure of Ge (111) implanted with Na^+ ions with $E_0 = 0.5$ keV at $D = 6 \cdot 10^{16}$ cm^{-2} before and after annealing

Parameter	Ge	$Na^+ \rightarrow Ge$	
		$T = 300$ K	$T = 850$ K
Φ	5.1	2.4	3.85
φ	4.7	2.4	3.8
χ	4	2.4	3.4
E_g	0.7	0	0.45

Note. Parameters of energy bands were determined with an error of ~ 0.05 eV.

I is taken from the straight-line section of $I(h\nu)$. It can be seen that $R_{Ge} = 0.22$ and $R_{NaGe_2} = 0.26$.

The main macroscopic parameters of „pristine“ and ion-implanted Ge were determined by analyzing these spectra (Table 2). It follows from Table 2 that the emergence of a narrow n-type band near E_c in ion-implanted Ge results in a reduction in the averaged value of E_g, which drops to ~ 0.2 eV. The properties of near-surface layers become closer to the characteristic of metals. A p-type narrow-band $NaGe_2$ semiconductor with bandgap width $E_g = 0.45$ eV forms after annealing.

Thus, the effect of Na^+ ion implantation and subsequent annealing on the composition and the electronic structure of surface layers of single-crystal Ge (111) has been examined for the first time. It was demonstrated that approximately 60–70 at.% of sodium form various compounds with Ge atoms in the process of ion implantation, while the rest of Na atoms remain unbound, leading to „metallization“ of ion-implanted layers. A uniform highly stoichiometric $NaGe_2$ film with a thickness of ~ 25–30 Å formed after annealing at $T = 800$ K. The energy-band parameters and densities of states of valence electrons of $NaGe_2$ nanofilms have been determined for the first time.

Conflict of interest

The authors declare that they have no conflict of interest.

References

[1] S.K. Ray, S. Das, R.K Singha, S. Manna, A. Dhar, Nanoscale Res. Lett., **6**, 224 (2011). DOI: 10.1186/1556-276X-6-224
[2] S. Das, K. Das, R.K. Singha, A. Dhar, S.K. Ray, Appl. Phys. Lett., **91** (23), 233118 (2007). DOI: 10.1063/1.2821114
[3] K. Das, M. NandaGoswami, R. Mahapatra, G.S. Kar, A. Dhar, H.N. Acharya, S. Maikap, J.-H. Lee, S.K. Ray, Appl. Phys. Lett., **84** (8), 1386 (2004). DOI: 10.1063/1.1646750
[4] J.-Y. Zhang, Y.-H. Ye, X.-L. Tan, X.-M. Bao, Appl. Phys. A, **71** (3), 299 (2000). DOI: 10.1007/s003390000518
[5] M.H. Liao, C.-Y. Yu, T.-H. Guo, C.-H. Lin, C.W. Liu, IEEE Electron Dev. Lett., **27** (4), 252 (2006). DOI: 10.1109/LED.2006.870416
[6] G.A. Maksimov, Z.F. Krasil'nik, D.O. Filatov, M.V. Kruglova, S.V. Morozov, D.Yu. Remizov, D.E. Nikolichev, V.G. Shengurov, Phys. Solid State, **47** (1), 22 (2005). DOI: 10.1134/1.1853436.
[7] D. Cooper, A. Béché, J.M. Hartmann, L. Hutin, C. Le. Royer, J.L. Rouviere, J. Phys.: Conf. Ser., **326**, 012025 (2011). DOI: 10.1088/1742-6596/326/1/012025
[8] R.G. Valeev, V.M. Vetoshkin, D.V. Surnin, Khim. Fiz. Mezoskopiya, **11** (2), 204 (2009) (in Russian). https://www.elibrary.ru/item.asp?id=18248341
[9] G.N. Kamaev, V.A. Volodin, G.K. Krivyakin, Tech. Phys. Lett., **47**, 609 (2021). DOI: 10.1134/S1063785021060237
[10] N. Fourches, IEEE Trans. Electron Dev., **64** (4), 1619 (2017). DOI: 10.1109/TED.2017.2670681
[11] R.I. Batalov, V.V. Vorobev, V.I. Nuzhdin, V.F. Valeev, R.M. Bayazitov, N.M. Lyadov, Yu.N. Osin, A.L. Stepanov, Tech. Phys., **61** (12), 1861 (2016). DOI: 10.1134/S1063784216120069.
[12] O.N. Gorshkov, I.N. Antonov, M.E. Shenina, A.Yu. Dudin, A.P. Kasatkin, Vestn. Nizhegorod. Univ., No. 4-1, 38 (2010) (in Russian). https://cyberleninka.ru/article/n/formirovanie-nanorazmernyh-chastits-zolota-v-tonkih-amorfnyh-plenkah-dioksida-germaniya-metodom-ionnoy-implantatsii/viewer
[13] A.L. Stepanov, V.V. Vorob'ev, V.I. Nuzhdin, V.F. Valeev, Yu.N. Osin, Tech. Phys. Lett., **44** (4), 354 (2018). DOI: 10.1134/S1063785018040260.
[14] D.A. Tashmukhamedova, B.E. Umirzakov, M.A. Mirdzhalilova, Izv. Ross. Akad. Nauk. Ser. Fiz., **68** (3), 424 (2004) (in Russian). https://www.elibrary.ru/item.asp?id=17641066
[15] D.A. Tashmukhamedova, B.E. Umirzakov, E.U. Baltaev, Poverkhn.: Rentgenovskie, Sinkhrotronnye Neitr. Issled., No. 8, 101 (2003) (in Russian). https://www.elibrary.ru/item.asp?id=17316038
[16] D.A. Tashmukhamedova, M.B. Yusupjanova, A.K. Tashatov, B.E. Umirzakov, J. Surf. Investig., **12** (5), 902 (2018). DOI: 10.1134/S1027451018050117.
[17] D.A. Tashmukhamedova, Bull. Russ. Acad. Sci. Phys., **70** (8), 1409 (2006).
[18] B.E. Umirzakov, D.A. Tashmukhamedova, A.K. Tashatov, N.M. Mustafoeva, D.M. Muradkabilov, Semiconductors, **54** (11), 1424 (2020). DOI: 10.1134/S1063782620110263.
[19] A.V. Kacyuba, A.V. Dvurechenskii, G.N. Kamaev, V.A. Volodin, A.Y. Krupin, Mater. Lett., **268** (6), 127554 (2020). DOI: 10.1016/J.MATLET.2020.127554